Absolute cross-section measurements for electron-impact ionization of Al^+, Cd^+, and Hg^+

D. S. Belic,* R. A. Falk,† C. Timmer, and G. H. Dunn‡

*Joint Institute for Laboratory Astrophysics, University of Colorado and National Bureau of Standards,
Boulder, Colorado 80309-0440*
(Received 2 February 1987)

Absolute cross sections for single ionization of Al^+, Cd^+, and Hg^+ by electron impact have been measured for electron energies from threshold to 2 keV using the crossed-beams technique. The Al^+ cross section shows a peak value of $(74\pm6)\times10^{-18}$ cm^2 at about 46 eV. In addition, for Al^+ there is significant structure around 80 eV, an energy corresponding to the $2p^53s^2nl$ autoionizing states of Al^+. The Cd^+ and Hg^+ cross sections show no major structures and have peak values of $(147\pm6)\times10^{-18}$ cm^2 and $(169\pm5)\times10^{-18}$ cm^2, respectively, both at an electron energy of roughly 100 eV. Comparisons are made to semiempirical and theoretical predictions and to other existing experimental data.

I. INTRODUCTION

Electron-impact ionization of positive ions plays an important role in physical phenomena ranging from discharges to high-temperature stellar and fusion-related laboratory plasmas, and has long been studied experimentally[1] and theoretically.[2] However, only a limited number of experiments have been done. Less than 70 ions have been studied in absolute experiments, mostly light ions in lower-charge states and only a few of those have had more than one outer-shell electron. On the theoretical side, full quantum descriptions of the process have only recently been developed and applied successfully in a number of cases and a few families of ions. Such treatments are complicated by the many-body nature of the process and by the necessity to include a number of physical mechanisms which can contribute to the ionization cross section in the case of complex species.

In addition to the direct knockout of an outer- or inner-shell electron, the ionization process may proceed via intermediate excitation of an inner-shell electron to a quasidiscrete state lying in the continuum, followed by autoionization. This process of excitation autoionization gives rise to a sharp onset in the ionization cross section at the excitation energy. The magnitude of these contributions depends on the excitation collision strength and on the branching ratio between radiative stabilization and autoionization of the quasibound intermediate state; in many cases these excitation-autoionization features are quite prominent. Another indirect-ionization process is dielectronic capture of the incident electron into a doubly-excited resonant state followed by double autoionization or, though probably less likely, by auto-double-ionization. Energetically, this occurs as a series of resonances below each of the excitation-autoionization onsets.

Until the past few years, most theoretical work has been oriented to describing direct-ionization cross sections. Numerous semiempirical and scaling-law prescriptions[3] have been developed for estimating cross sections. A quite successful one and probably the most widely used is the Lotz[4] formula which gives (with a suggested accuracy of $+40, -30\%$) the direct-ionization cross section versus energy (in cm^2) in the form

$$S(E) + \sum_i^N \frac{a_i n_i}{EP_i} \ln(E/P_i)\{1 - b_i \exp[-c_i(E/P_i - 1)]\} .$$

(1)

Here N is the number of subshells contributing to ionization, n_i is the number of electrons in subshell i, P_i is the ionization energy for that subshell (in eV) and a_i, b_i, and c_i are empirical coefficients for different subshells. Constants b_i and c_i are introduced to correct the position of the peak of the cross section and should have only a minor influence on its magnitude. However, in cases of many-electron shells, these coefficients can lead to considerably reduced cross sections. Therefore, numerous users simply neglect these constants by setting them to zero. In addition, they often choose a_i to be "universal" and equal to 4.5×10^{-14} cm^{2}eV^2 for all subshells and all species. Some qualitative aspects of such a simplified Lotz formula will be discussed later when compared with our measurements.

Recently, several quantum-mechanical methods for calculating direct-ionization cross sections have been developed.[2] Methods such as the scaled plane-wave Born (SPWB),[5] Coulomb-Born (CB), Coulomb-Born-exchange (CBE),[6] distorted-wave (DW), and distorted-wave-exchange (DWE)[7] have been successfully applied in describing the ionization of some specific ions and a few isoelectronic sequences. The use of close-coupling (CC) wave functions to represent the initial and final states of the ions[8] has been implemented in a few cases. Still, for heavy, many-electron ions, further theoretical development is necessary.

A significant contribution of excitation autoionization to ionization has been observed for most of the alkali-metal sequences, the Mg isoelectronic sequence, and a sizable number of other ions. Detailed discussions of its significance are given by Crandall,[9] Crandall et al.,[10] Falk et al.,[11] Howald et al.,[12] and many others.[1,2] The contribution from excitation autoionization, which in some

cases may be more than an order-of-magnitude larger than direct ionization, has been accounted for theoretically by adding the appropriate excitation cross section to that of the direct process. Such calculations in the DW and R-matrix CC approximation, taking into account a number of states and branching ratios, have well-described[13,14] recent experimental measurements[12] on the Mg isoelectronic sequence.

In this paper we present experimental data on electron-impact ionization of Al^+, Cd^+, and Hg^+ ions. The first one, Al^+, is the first member of the Mg isoelectronic sequence which has been recently treated both experimentally[12] and theoretically,[13,14] and it seems to be understood. Heavy, many-electron ions have not been studied nearly as much, and discrepancies are found between experimental measurements and various predictions.

II. EXPERIMENTAL TECHNIQUE

The measurements were performed using a crossed-beams technique with an apparatus that has been previously described.[15] The beams of variable-energy electrons and mass-analyzed ions intersect at a right angle in an ultrahigh-vacuum environment. The product (doubly-charged) ions are separated from the primary (singly-charged) ions in a parallel-plate electrostatic analyzer and directed to an electron multiplier where they are individually counted. The ionization cross sections at energy E are determined from measured parameters by[1,16]

$$\sigma(E) = \frac{R}{I_e I_i} \frac{e^2 v_e v_i}{(v_e^2 + v_i^2)^{1/2}} \frac{F}{D_{2+}}, \tag{2}$$

where R is the product ion-count rate, I_e and I_i are the electron and ion-beam currents, respectively, v_e and v_i are the electron and ion velocities, e is the charge of an electron, F is a geometrical factor taking into account the spatial overlap of the two beams, and D_{2+} is the detection efficiency for the product doubly-charged ions.

The ions were produced in a commercially available,[17] hot cathode-discharge ion source. For the Al^+ and Cd^+ experiments, pure Al or Cd metal was inserted into the source, while for the Hg^+ experiment a sample of HgO_2 was introduced. In all three cases, after passing ion-collimation optics and the 60° sector magnet for mass separation, stable beams of a few hundred nA (at 2 keV) were obtained and crossed in the interaction region with a magnetically confined electron beam.[18] At the intersection point, beam profiles were determined by using a movable probe with a narrow slit. Beam currents were measured using biased Faraday cups and calibrated electrometers. Background signals were separated from the total signals by chopping the electron beam while one counter recorded signal plus background and another recorded background only. The electron energies at which data were taken were corrected for space-charge and ion-beam velocity effects.

The detection efficiencies for the product ions were determined in separate experiments. A benchmark energy of approximately 100 eV was chosen at which to make the absolute measurements, and the electron multiplier was turned into a Faraday cup to relate the number of counts to the charge hitting the detector. The current was measured by a sensitive, vibrating-reed electrometer. This procedure yielded a detection efficiency of 0.78 for Al^{2+}, 0.67 for Cd^{2+}, and 0.70 for Hg^{2+} ions.

Measurements at other energies were taken by counting signal ions at a given energy for a specific time, moving to another energy in a scan mode, and repeating the scan many times for a data set. During each scan, the benchmark energy was included so that all points could be put on an absolute scale. Profiles for calculating beam overlaps were obtained contiguous to the measurement run. Cross sections at each energy were determined from averages of results from four or more such measurement runs. Good agreement was obtained between the standard deviation of the mean of the averages and counting statistics. Thus counting statistics (corresponding to one standard deviation) were taken as representative of relative uncertainties. Total absolute uncertainties, on the other hand, were found by adding the relative uncertainties in quadrature to the standard deviation of the absolute measurement of the cross section (at the benchmark energy) and to the estimated systematic uncertainties, which are shown in Table I.

TABLE I. Experimental uncertainties (67% confidence level).

Absolute calibration uncertainties at benchmark energy (>100 eV)	Al^+	Cd^+	Hg^+
Statistical	4.6	1.4	1.2
Vibrating-reed electrometer calibration	2.0	2.0	2.0
Leakage resistance	1.0	1.0	1.0
Transmission of analyzer	1.0	1.0	1.0
Form factor	2.0	2.0	2.0
Electron path length	1.0	1.0	1.0
Electron-beam current measurement	1.5	1.5	1.5
Ion-beam current measurement	1.5	1.5	1.5
Uncollected electron current	1.0	1.0	1.0
Quadrature sum	9%	5.5%	5%

III. RESULTS AND DISCUSSION

A. Al$^+$

The measured cross sections versus electron energy for electron-impact ionization of Al$^+$ are tabulated in Table II and shown in Fig. 1 (solid circles). The solid error bars indicated in the figure are relative uncertainties due to counting statistics at the one standard-deviation level. The dashed bar represents the total uncertainty for the point at the cross-section peak. The most interesting feature in the cross-section curve is the abrupt change in the magnitude at about 75 eV with an estimated magnitude of approximately 5×10^{-18} cm^2, or 7% of the total cross-section peak value. This structure is identified as being due to $2p^63s^2$-$2p^53s^2nl$ inner-shell excitation followed by autoionization (characteristic for the Mg isoelectronic sequence[12]) and will be discussed in more detail later.

Comparison of our data is made to several theoretical results and other experimental measurements. The only other experimental results, due to Montague and Harrison,[19] for Al$^+$ ionization are also shown in Fig. 1.

Montague and Harrison estimated 9% of metastable ions in their target-ion beam and have corrected their measured data for this presence. The correction changed their cross-section values on the order of 2%. Figure 1 shows their derived ground-state cross sections. The two measurements are in excellent agreement as to the magnitude of the peak value of the cross section, but the Montague and Harrison results lie considerably below the present data at all energies above the peak. In the recent paper by Tayal and Henry,[14] this discrepancy was explained by suggesting the presence of metastable ions in our experiment as well. However, this seems unlikely to us, since we have estimated on the basis of measurements below the energy threshold for ground-state ionization, to have only 3% (and a maximum of 7%) of our ion beam in the metastable $2p^63s3p$ state. The correction of our data due to metastable presence would be less than 0.7%, compared to the apparent 15–20 % differences seen in Fig. 1. The data of Montague and Harrison do not show the structure near 75 eV due to excitation autoionization. We do not have an explanation for these discrepancies. Special care was dedicated to electron-energy calibration and

TABLE II. Measured cross section (σ) for single ionization of Al$^+$ by electron impact. $\Delta\sigma_r$ is relative uncertainty as counting statistics at 1 standard deviation of the mean. $\Delta\sigma_a$ is total uncertainty (Table I).

| E (eV)	σ	$\Delta\sigma_r$ (10^{-18} cm^2)	$\Delta\sigma_a$	E (eV)	σ	$\Delta\sigma_r$ (10^{-18} cm^2)	$\Delta\sigma_a$
19.0	3.8	1.6	1.6	68.9	66.5	1.0	6.1
20.0	12.6	1.6	2.0	70.7	67.2	1.0	6.1
20.9	20.0	1.8	2.5	72.7	66.3	1.0	6.0
22.8	36.8	1.5	3.7	74.6	66.1	1.1	6.1
23.8	40.8	1.9	4.1	76.6	67.2	1.1	6.2
24.7	49.5	1.5	4.7	78.5	67.0	1.1	6.1
25.8	51.2	1.5	4.9	80.4	67.8	2.0	6.4
26.7	52.8	1.9	5.1	82.2	67.8	2.0	6.4
27.7	56.6	1.9	5.4	84.2	65.9	2.0	6.3
28.6	61.3	1.4	5.7	86.1	65.5	2.0	6.2
30.4	67.2	2.3	6.5	106.5	58.8	0.8	5.3
34.3	71.2	1.8	6.7	125.9	54.8	0.6	5.0
36.2	70.7	1.8	6.6	145.6	51.4	0.6	4.7
38.2	72.2	1.7	6.7	165.3	48.8	0.5	4.4
40.0	73.1	1.7	6.8	185.0	45.1	0.5	4.1
42.0	73.1	1.7	6.8	204.5	41.5	0.5	3.8
43.9	72.0	1.5	6.7	223.6	38.3	0.4	3.5
45.8	74.5	1.4	6.9	243.1	35.8	0.4	3.2
47.8	73.1	1.4	6.7	262.5	33.5	0.4	3.0
49.7	72.4	1.4	6.7	281.8	31.8	0.3	2.9
51.6	72.9	1.2	6.7	301.3	30.9	0.3	2.8
53.5	72.6	1.2	6.6	320.8	29.9	0.3	2.7
55.5	71.4	1.2	6.5	340.3	28.8	0.3	2.6
57.4	70.8	1.2	6.5	359.8	27.8	0.3	2.5
59.4	69.9	1.2	6.4	378.8	27.0	0.3	2.5
61.2	69.5	1.2	6.4	588.0	21.7	0.4	2.0
63.2	68.8	1.0	6.3	787.0	18.0	0.3	1.7
65.1	68.0	1.0	6.2	990.0	15.0	0.3	1.4
66.9	67.6	1.0	6.2				
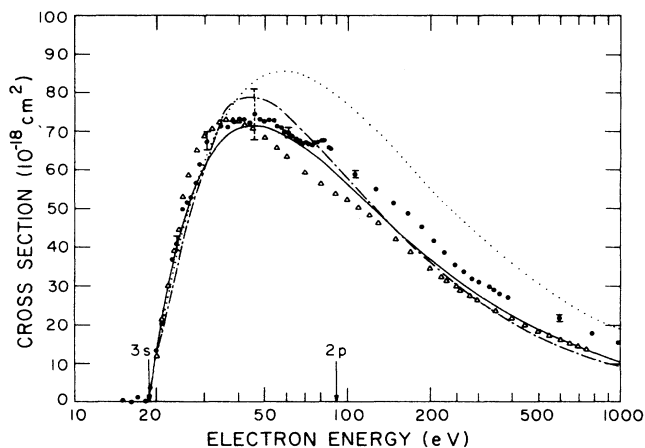
FIG. 1. Cross section vs energy for electron-impact ionization of Al$^+$ (●). Representative relative uncertainties are shown as the solid bars and the peak-value absolute uncertainty is shown by the dashed error bar. Experiment of Montague and Harrison (Ref. 19), △; Lotz semiempirical formula, Eq. (1), · · · ·; SPWB, McGuire (Ref. 3), —·—·—·; and DWE Younger (Ref. 5), result for Ar^{6+} scaled to Al$^+$, ———. Arrows indicate threshold energies for ejection of electrons from various subshells.

total-signal collection in the present measurements. We also lowered the electron emission from the cathode, thus lowering the electron-energy spread, to be able to isolate the structure in the cross section.

Comparison with the prediction of the semiempirical Lotz formula, Eq. (1), is of interest, since this formula is heavily relied upon by various authors and user groups. Subshell ionization energies calculated by Griffin[20] are listed in Table III. For the outer-shell electrons, the experimental values (in parentheses) were used. Ionization of the 2p shell has not been included in constructing the Lotz curve, since the $1s^2 2s^2 2p^5 3s^2$ configuration lies above the $1s^2 2s^2 2p^6$ configuration, and ejecting an electron in the 2p shell would lead to double ionization. In Fig. 1 the dotted curve represents the result with all coefficient values as originally recommended by Lotz, for the 3s subshell only. This estimate is larger than the measured cross sections for all energies above the peak by as much as 40%; but still, the agreement is within the originally suggested accuracy. By using the universal value of 4.5×10^{-14} cm^{2}eV^2 with $b_i = c_i = 0$, the resulting cross section peaks at 50 eV, with an additional 30% higher

value. When one takes a_i as recommended by Lotz and $b_i = c_i = 0$, cross sections are somewhere in between those two limits, reproducing the peak position better but being higher than the measurements by about 20%. The Lotz formula also leads to overestimates of direct cross sections for other members of the Mg isoelectronic sequence[12] (S^{4+}, Cl^{5+}, and Ar^{6+}) by 20–30%.

Also included in the figure (dot-dash curve) is the result from the scaled plane-wave Born approximation due to McGuire[5] evaluated for the 3s subshell. The agreement with our measurement is reasonable over a wide energy range, particularly if excitation autoionization is accounted for as discussed below.

The direct-ionization cross section for Mg-like Ar^{6+} ion has been calculated in the DWE approximation by Younger.[21] That result may be scaled along the isoelectronic sequence, thereby to obtain results for Al$^+$, by the prescription

$$\sigma(E) = \frac{(124.3)^2}{E_I^2} f(E/E_I) , \tag{3}$$

where E is electron energy in eV, 124.3 eV is the ionization energy of Ar^{6+}, E_I is the ionization potential (in this case, $E_I = 18.2$ eV) of the ion in eV and $f(E/E_I)$ is the cross section given by Younger for ground-state Ar^{6+} as a function of the electron energy in ionization threshold units. It has been pointed out[22] that the actual scaling along the isoelectronic sequence is not exactly as given here, but for some ions from this sequence (S^{4+}, Cl^{5+}), as shown by Howald et al.,[12] and also Al$^+$, as already shown by Tayal and Henry,[14] the agreement with experimental data is excellent. This also may be seen from the solid curve in Fig. 1 for direct ionization of Al$^+$. However, it should be noted that Younger's direct-ionization cross sections for Ar^{6+} are about 15% less than the experimental data of Howald et al.[12] before the onset of the indirect processes. That trend may explain cross sections obtained from the scaling procedure that are slightly lower than our measured data.

To examine the effect of excitation autoionization, Fig. 2 shows the cross sections for the energy range 50–300 eV on an expanded vertical scale. The contribution to the ionization cross section from excitation autoionization can be isolated by subtracting the cross section for direct ionization. For the purpose of this subtraction, the scaled DWE cross section discussed above was multiplied by 1.02 to give a good fit to the experimental data just below threshold for excitation of 2p electrons. This is shown as

TABLE III. Shell-ionization energies for Al$^+$, Cd$^+$, and Hg$^+$ as calculated by Griffin.[20]

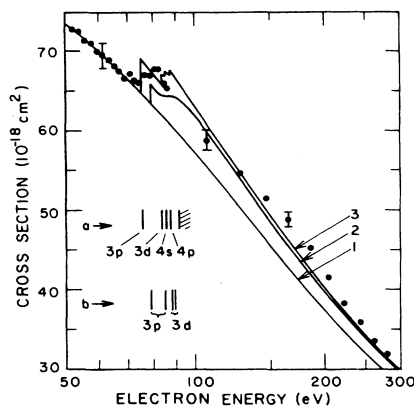| | Al$^+$ | | Cd$^+$ | | Hg$^+$ |
Shell	Energy (eV)	Shell	Energy (eV)	Shell	Energy (eV)
3s	18.2 (18.82)	5s	16.2 (16.9)	6s	17.8 (18.75 expt.)
2p	91.5	4d	26.5	5d	24.3
		4p	90.5	5p	89.3
		4s	133.9	4f	117.2
		3d	424.5	5s	144.0
		3p	648.8		

FIG. 2. Cross section for Al^+ ionization in 50–300 eV region emphasizing the excitation-autoionization contribution. Experimental points are as in Fig. 1. Curve 1 is DWE Younger result (see text, Fig. 1) multiplied by 1.02 to fit experimental data below the threshold for indirect processes. Curve 2 is R-matrix calculation by Tayal and Henry (Ref. 14) added onto curve 1. Curve 3 is obtained by scaling, Griffin et al. DWE data (Ref. 23) for Al^{2+} excitation added onto curve 1, see text. The energy levels shown here are the same as in Table IV: (a) Griffin, and (b) Tayal and Henry.

curve 1 in Fig. 2. The excitation cross sections resulting from the subtraction have magnitudes in the range $(3-5)\times10^{-18}$ cm^2 for electron energies 80–200 eV, as can be seen in the figure. Comparison can be made with a variety of calculations and estimates of the excitation cross sections.

First, Tayal and Henry[14] have recently made direct calculations of this effect for Al^+ as well as for other Mg-like

TABLE IV. Excitation energies of the autoionizing states of Al^+ relative to the ground state (in eV).

State	Griffin (Ref. 20) (averaged)	Tayal and Henry (Ref. 14)
$1s^22s^22p^53s^23p$	75.4	^3S 78.76
		^3D 79.62
		^1D 80.11
		^3P 80.19
		^1P 80.19
		^1S 84.95
$3d$	84.0	$^3P°$ 88.27
		$^3F°$ 89.39
		$^1F°$ 89.42
		$^3D°$ 89.54
		$^1D°$ 89.54
		$^1P°$ 89.51
$4s$	83.6	$^3P°$ 88.27
		$^1P°$ 88.69
$4p$	85.4	
$4d$	87.6	

ions using the R-matrix approach. Their results are shown as curve 2 in Fig. 2, and it can be seen that the agreement is really quite good as far as the magnitude of the effect is concerned. There seems to be, however, a shift in the energy at which the effect onsets. Figure 2 shows excitation energies as calculated by Tayal and Henry[14] (series b) and also energies as calculated by Griffin[20] (series a), and the Griffin results are in better agreement with the observed onsets. This systematic difference in energies was also observed[12–14] for other Mg-like ions.

As another means of getting a comparison with the excitation cross section, one can assume that there is essentially no difference in exciting the $2p$ electrons of Al^+ ($1s^22s^22p^63s^2$) or the $2p$ electrons of Al^{2+} ($1s^22s^22p^63s$)—i.e., the $3s$ electrons are just spectators in the process and it does not matter whether there are one or two spectators. With that assumption, one can simply look at the previously calculated[23,24] cross sections for the excitation of the $2p$ electrons of Al^{2+}, add them to the DWE direct-ionization curve in Fig. 2, and compare them with the experiment. This is done in curve 3 of Fig. 2, where the calculation of Griffin et al.[23] was used for Al^{2+}. Again, agreement is good. It should be noted that in using the results of Griffin et al. only the threshold values of cross sections were taken from their paper. These were then given a continuing analytic form of $(A/E)\ln E$ or A/E, respectively, depending on whether the state optically connects or not with the $2p$ electrons being excited. Recently, Griffin[20] has used the DWE approximation to calculate the cross section for the $2p$ electron excitation of Al^+, and obtained results for excitation autoionization which are in excellent agreement with values from the above described estimate, well within 10%.

McGuire[25] calculated the excitation of the $2p$ electrons of Al^+ using the SPWB method. However, the SPWB method does not give rise to the finite cross section at threshold characteristic of the Coulomb potential, and the feature is "washed out." His results can, however, be used to obtain the oscillator strength by looking at his data at high energies. This oscillator strength can then be used in conjunction with the Gaunt-factor formula[26] to get an estimate of the excitation. This will account only for the transitions that connect optically with the $2p$ electrons being excited. This effort yields a cross section at 75 eV of about 1.7×10^{-18} cm^2, a value somewhat smaller than observed, but expectedly so since only the optically allowed states are accounted for.

In the work[12,13] on other Mg-like ions, it was found that inner-shell ionization of $2p$ electrons had to be taken into account to obtain agreement between experiment and theory. In those cases, the beams contained a substantial fraction of metastable ions in $2p^63s3p$ configurations. Ionization of a $2p$ electron from the metastable gives configurations which are long-lived against autoionization, hence the products are counted for single ionization— even though they eventually lead to double ionization. In this work on Al^+ there do not seem to be significant numbers of the target ions in the metastable levels. We have pointed out earlier that in this experiment about 3% of the ions can be in the $2p^63s3p$ state (with an upper lim-

it of 7%). With the Lotz formula, we estimated, using this fraction, the contribution via $2p$ ionization to be of the order of 2.7×10^{-19} cm^2. Taking into account the recently calculated[20] autoionization branching ratio of 50% for the $2p^5 3s3p$ state, the contribution is approximately 1.4×10^{-19} cm^2, and if the maximum 7% metastable population is assumed, the contribution could be up to 3.3×10^{-19} cm^2. Both in the present data and in the data of Montague and Harrison,[19] there is a broad structure between 90- and 200 eV—just the energy range where inner-shell ionization might be in evidence. By continuing a smooth curve from above and below this feature, one can estimate the magnitude to be about $(2-4) \times 10^{-18}$ cm^2. This is more than an order of magnitude greater than can be accounted for by inner-shell ionization of metastable targets as just discussed. Inner-shell ionization of the ground state will lead to the $2p^5 3s^2$ configuration which should autoionize with nearly unity branching[20] to give double ionization—and so there should be no contri-

bution to the cross section here. The experimental evidence appears strong, however, that there is an additional mechanism operating in this energy range. There is a genuine dilemma as to what one may attribute it to.

B. Cd$^+$ and Hg$^+$

The measured cross sections versus electron energy for single ionization of Cd$^+$ and Hg$^+$ are listed in Tables V and VI, respectively, including relative and absolute uncertainties. The results are also shown graphically in Figs. 3 and 4 (solid circles). A few representative relative error bars are shown as well as the absolute error bar at the benchmark energy (dashed bar). As with Al$^+$, measurements below threshold for ionization from the ground state are not included in Tables V and VI but are included in Figs. 3 and 4. For Cd$^+$ the energies and cross sections are 13.7 eV, 0.07×10^{-18} cm^3; 14.7 eV, 0.46×10^{-18} cm^2; and 15.8 eV, 0.4×10^{-18} cm^2. For Hg$^+$ we have

TABLE V. Measured cross section for single ionization of Cd$^+$ by electron impact. Symbols are as described in Table II.

E (eV)	σ	$\Delta\sigma_r$ (10^{-18} cm^2)	$\Delta\sigma_a$	E (eV)	σ	$\Delta\sigma_r$ (10^{-18} cm^2)	$\Delta\sigma_a$
16.8	3.8	0.1	0.2	59.7	138.6	3.3	8.3
17.8	8.2	0.2	0.5	61.6	140.5	2.6	8.2
18.8	11.3	0.3	0.7	63.7	142.2	2.8	8.3
19.8	21.9	0.4	1.3	65.6	141.6	0.7	7.8
20.8	29.8	0.5	1.7	67.6	142.2	0.9	7.8
21.8	39.3	0.6	2.2	69.6	142.9	0.9	7.9
22.8	44.4	0.7	2.5	71.5	143.8	1.0	8.0
23.8	48.7	0.7	2.8	73.5	143.4	1.0	8.0
24.8	53.4	0.3	3.1	75.5	144.6	1.0	8.0
25.8	57.1	0.9	3.3	77.5	145.0	1.2	8.1
26.8	60.8	0.8	3.4	79.5	146.1	1.8	8.2
27.8	64.0	0.5	3.8	81.5	145.4	1.6	8.2
28.8	66.8	0.8	3.7	83.4	145.6	1.4	8.2
29.8	69.7	0.6	3.9	85.4	145.5	2.1	8.3
30.8	72.1	0.7	4.0	87.4	145.4	1.8	8.2
31.8	75.9	1.0	4.3	89.4	146.3	2.0	8.3
32.8	80.0	0.6	4.4	91.4	146.3	2.4	8.4
33.8	83.3	0.6	4.6	93.4	147.3	2.1	8.4
34.8	87.3	0.5	4.8	119.9	141.5	0.3	7.9
35.8	90.5	1.1	5.1	140.3	135.6	1.4	7.7
37.8	96.8	1.1	5.4	167.6	130.6	0.2	7.2
39.8	102.6	1.9	5.8	186.5	123.0	0.2	6.8
41.8	106.7	2.0	6.2	234.4	119.9	0.1	6.6
43.8	111.9	1.3	6.3	281.3	113.5	0.2	6.3
45.8	116.2	1.1	6.5	375.2	105.9	0.2	5.9
47.7	119.1	1.9	6.8	474.2	100.3	0.2	5.6
49.7	123.5	1.9	7.1	580.0	92.9	0.2	5.1
51.7	126.2	2.1	7.2	782.0	75.7	0.2	4.2
53.7	130.9	2.5	7.6	980.0	62.4	0.2	3.5
55.7	134.6	2.5	7.8	1490	39.5	0.5	2.2
57.7	136.0	2.7	8.0	1991	31.5	0.3	1.8

13.9 eV, 0.26×10^{-18} cm^2; 14.9 eV, 0.24×10^{-18} cm^2; 16 eV, 0.17×10^{-18} cm^2; 17 eV, 0.23×10^{-18} cm^2; and 18 eV, 0.28×10^{-18} cm^2. Based on these values below threshold we estimate that the maximum fraction of ions in excited (metastable) states in either the Cd$^+$ or Hg$^+$ beams is below 1%. Comparisons are made in the figures to semiempirical, existing theoretical results, and other experimental measurements.

The semiempirical Lotz formula, Eq. (1), has been applied in both cases, using subshell ionization energies listed in Table III (experimental values are available only for the outer-shell electrons). Only the first two subshells have been included in each case, since ionization energies for the others are above the threshold for double ionization. Interesting results are obtained using different values for the coefficients a_i, b_i, and c_i, which appear in Eq. (1). The plotted curves (dotted) for the Lotz predictions in Fig. 3 for Cd$^+$ and in Fig. 4 for Hg$^+$ are obtained by using all the coefficients as recommended origi-
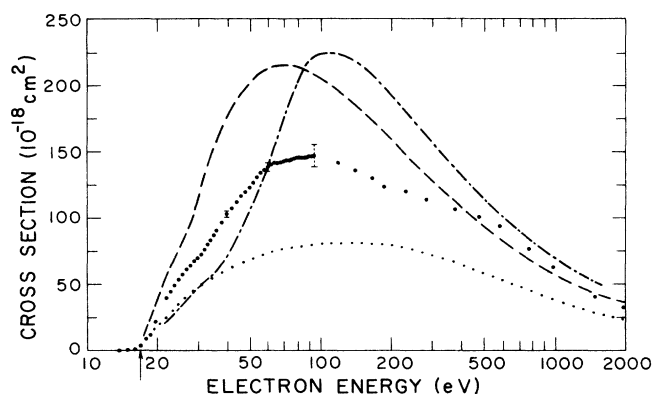

FIG. 3. Cross section for electron-impact ionization of Cd$^+$ vs energy. ●, present data; · · · ·, the Lotz prediction; — — —, semiempirical prediction from Drawin (Ref. 27) formula; and —·—·—·, SPWB from McGuire (Ref. 5), for $5s + 4d$ contribution.

TABLE VI. Measured cross section for single ionization of Hg$^+$ by electron impact. Symbols are as described in Table II.

| E (eV)	σ	$\Delta\sigma_r$ $(10^{-18}$ cm$^2)$	$\Delta\sigma_a$	E (eV)	σ	$\Delta\sigma_r$ $(10^{-18}$ cm$^2)$	$\Delta\sigma_a$
19	10.8	1.6	1.7	62	156.3	3.1	8.4
20	21.7	0.9	1.4	64	160.3	0.8	8.6
21	32.5	0.6	1.7	66	161.8	0.2	8.1
22	39.7	0.5	2.0	68	165.5	2.7	8.7
23	45.9	0.7	2.4	70	162.4	3.0	8.7
24	51.2	0.8	2.7	72	164.4	3.7	9.0
25	58.9	1.0	3.1	74	160.8	2.8	8.5
26	64.3	1.7	3.6	76	167.4	2.6	8.8
27	70.2	2.0	4.0	78	165.6	2.3	8.6
28	74.9	1.6	4.1	80	166.3	1.8	8.5
29	80.3	1.5	4.3	82	167.1	0.8	8.4
30	85.1	0.9	4.3	84	167.8	0.6	8.4
31	89.6	1.0	4.6	86	167.4	0.2	8.4
32	92.8	2.0	5.1	88	166.1	0.5	8.3
33	97.6	2.7	5.6	90	169.0	0.7	8.5
34	100.9	3.7	6.3	92	168.3	1.7	8.6
35	102.2	1.9	5.5	94	167.6	2.1	8.6
36	105.6	0.8	5.3	120	161.8	0.4	8.1
38	112.6	0.3	5.6	158	156.0	3.0	9.4
40	118.9	0.4	6.0	186	149.6	1.1	7.7
42	123.9	0.6	6.2	233	139.5	0.8	7.1
44	128.9	1.7	6.7	280	131.4	2.0	7.1
46	134.0	2.0	7.0	385	115.6	1.2	5.9
48	137.4	2.0	7.2	484	106.8	3.2	6.3
50	142.7	1.9	7.4	584	100.1	4.4	6.7
52	145.9	2.1	7.6	785	78.2	4.6	5.3
54	148.4	0.7	7.5	982	62.0	0.4	3.1
56	151.2	0.9	7.6	1474	43.6	2.1	2.4
58	154.3	1.6	7.9	1980	36.3	1.3	1.9
60	157.1	1.6	8.0				
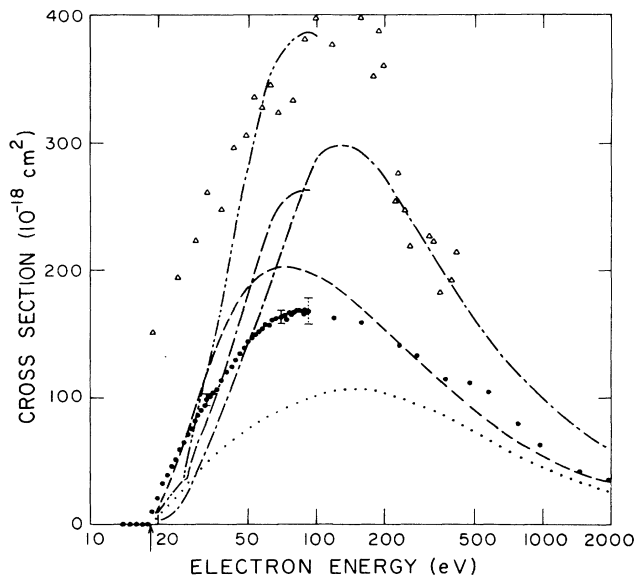
FIG. 4. Electron-impact ionization cross section for Hg^+ vs energy. ● present data; △, experimental, Kupriyanov et al. (Refs. 28 and 29); · · · ·, Lotz [Eq. (1)] prediction; — — —, Drawin (Ref. 27) prescription; —·—·—·, SPWB, McGuire (Ref. 5), for $6s + 5d$ subshells. --—-- and —————, Younger (Ref. 30) DWE, for $6s + 5d$ subshells, see text.

nally by Lotz. Both curves have substantial d inner-shell contributions, but in both cases measured cross sections are underestimated at the peak by more than 40%. Possible explanations for this disagreement deserve comment. Assuming that the Lotz coefficients are "good" in predicting direct ionization, then the measured cross sections may be higher due to the excitation-autoionization contribution. We do not have access to autoionizing energy levels or possible indirect-ionization cross-section magnitudes, and since structure is not evident in the curves we cannot pursue this point further. It is more likely that the coefficients deduced from the atomic mercury ionization data are not good for Hg^+ ionization.

We have tried to apply the universal a_i coefficients with $b_i = c_i = 0$ in Eq. (1). In this case, cross sections for both ions are nearly a factor of 2 higher around the peak, although they converge well to measured data at 2 keV. Using a similar approach, with $b_i = c_i = 0$, but with the originally recommended values for a_i (which are close to the universal a_i for s and p subshells, but about a half of that for d and f subshells) we have calculated cross sections which fit experimental data reasonably well over the entire energy range—within 20%. Based on this and our earlier experience[15] in reproducing measured cross sections for heavy-ion ionization by the Lotz formula, we are coming to the conclusion that the simplified version (with b_i and c_i set to zero) may be useful if instead of 4.5×10^{-14} for a_i one uses half of that value for the d and f subshells. Of course, much more analytical comparison

with experiments needs to be done in order to test this conclusion.

Measured cross sections have also been compared with the predictions of the semiempirical formula due to Drawin.[27] As can be seen from the figures, these results (dashed curves) agree fairly well with the Hg^+ data, but the predictions for Cd^+ are larger than the measured cross section by more than 50% for low energies.

There apparently are no other experimental measurements on Cd^+ ionization. Other experimental results for Hg^+ ionization, due to Kupriyanov et al.,[28,29] are shown as open triangles in Fig. 4 and are roughly a factor of 2 higher than the present results. However, it can be seen from the figure that they present a nonzero cross section at the ionization threshold. With the zero offset subtracted from the Kupriyanov data, much better agreement with the present measurement can be achieved.

Also included (dot-dashed curves) in the graphs for Cd^+ and Hg^+ are calculations using the SPWB approximation due to McGuire.[5] Cross sections estimated this way are small at low energies and overestimated by as much as 70%, at high energies.

Quantum calculations were performed by Younger[30] for Hg^+ ionization and his results are shown in Fig. 4. The upper Younger curve (--—---) is obtained by using a "standard" distorted-wave Born-exchange (DWBE) approximation. The curve is dominated by the $5d$ contribution which is in turn dominated by the $5d^9kf$ ejection channel. The reason for this large kf contribution is the neglect of the important term dependence in the $5d^9kf\,^1P$ channel. Essentially, the $5d$-kf exchange interaction results in a double-well potential for the continuum electron with a potential barrier in the vicinity of the $5d$ subshell. At low-ejected energies, the kf partial wave cannot penetrate the barrier, and cannot achieve a large overlap with the $5d$ orbital which results in a smaller cross section. The lower curve (—————) predicted by Younger shows the effect of considering ejected channel dependence. The cross section is reduced considerably, although it is still not in agreement with experimental data. Part of the residual disagreement is expected to be due to ground-state correlation of the form $5d^{10}$-$5d^8 4f^2$. Younger[30] has pointed out that one should also consider the effect of polarizability of the $6s$ orbital in determining the ejected wave function, an effect not included in his term-dependent potential.

Obviously, further theoretical work is needed in order to achieve a better description of ionization cross sections for many-electron systems.

ACKNOWLEDGMENTS

*Permanent address: Department of Physics and Metrology, University of Beograde, P.O. Box 550, Beograd, Yugoslavia.

†Permanent address: Boeing Aerospace Co., Seattle, WA 98124.

‡Also at Quantum Physics Division, National Bureau of Standards.

[1]For a recent review, see G. H. Dunn, in *Electron Impact Ionization*, edited by T. D. Mark and G. H. Dunn (Springer-Verlag, New York, 1985), p. 277.

[2]For a recent review see S. M. Younger, in *Electron Impact Ionization*, edited by T. D. Mark and G. H. Dunn (Springer-Verlag, New York, 1985), p. 1.

[3]For a recent review see S. M. Younger and T. D. Mark, in *Electron Impact Ionization*, edited by T. D. Mark and G. H. Dunn (Springer-Verlag, New York, 1985), p. 24.

[4]W. Lotz, Z. Phys. **216** 241 (1968); **220**, 466 (1969).

[5]E. J. McGuire, Phys. Rev. A **3**, 267 (1971); **16**, 62 (1977); **20**, 445 (1979).

[6]R. E. H. Clark and D. H. Sampson, J. Phys. B **17**, 3311 (1984); L. B. Golden and D. H. Sampson, *ibid*. **13**, 2645 (1980); D. L. Moores, L. B. Golden, and D. H. Sampson, *ibid*. **13**, 385 (1980).

[7]S. M. Younger, Phys. Rev. A **24**, 1278 (1981); **24**, 1272 (1981); **23**, 1138 (1981); **22**, 1425 (1980).

[8]H. Jakubowicz and D. L. Moores, J. Phys. B **14**, 3733 (1981).

[9]D. H. Crandall, Phys. Scr. **23**, 153 (1981).

[10]D. H. Crandall, R. A. Phaneuf, R. A. Falk, D. S. Belic, and G. H. Dunn, Phys. Rev. A **25**, 143 (1982).

[11]R. A. Falk, G. H. Dunn, D. C. Griffin, C. Bottcher, D. C. Gregory, D. H. Crandall, and M. S. Pindzola, Phys. Rev. Lett. **47**, 494 (1981).

[12]A. M. Howald, D. C. Gregory, F. W. Meyer, R. A. Phaneuf, A. Muller, N. Djuric, and G. H. Dunn, Phys. Rev. A **33**, 3779 (1986).

[13]M. S. Pindzola, D. C. Griffin, and C. Bottcher, Phys. Rev. A **33**, 3787 (1986).

[14]S. S. Tayal and R. W. Henry, Phys. Rev. A **33**, 3825 (1986).

[15]W. T. Rogers, G. Stefani, R. Camilloni, G. H. Dunn, A. Z. Msezane, and R. J. W. Henry, Phys. Rev. A **25**, 737 (1982).

[16]K. T. Dolder and B. Peart, Rep. Prog. Phys. **39**, 93 (1976).

[17]M. Menzinger and L. Wahlin, Rev. Sci. Instrum. **40**, 102 (1969).

[18]P. O. Taylor and G. H. Dunn, Phys. Rev. A **18**, 2304 (1973).

[19]R. G. Montague and M. F. A. Harrison, J. Phys. B **16**, 3045 (1983).

[20]D. C. Griffin (private communication).

[21]S. M. Younger, At. Data Fusion **7**, 190 (1981); Controlled Fusion Atomic Data Center Newsletter, Oak Ridge National Laboratory (unpublished).

[22]S. M. Younger, Phys. Rev. A **22**, 111 (1980).

[23]D. C. Griffin, C. Bottcher, and M. S. Pindzola, Phys. Rev. A **25**, 154 (1982).

[24]R. J. W. Henry and A. W. Msezane, Phys. Rev. A **26**, 2545 (1982).

[25]E. J. McGuire (private communication).

[26]H. Van Regermorter, Astrophys. J. **136**, 906 (1962).

[27]H. W. Drawin, in *Plasma Diagnostics*, edited by W. Lochte-Holtgreven (North-Holland, Amsterdam, 1968), p. 842. See also Z. Phys. **164**, 513 (1961); **168**, 238 (E) (1962).

[28]S. E. Kupriyanov and Z. Z. Latypov, Zh. Eksp. Teor. Fiz. **18**, 558 (1964) [Sov. Phys.—JETP **45**, 815 (1963)].

[29]Z. Z. Latypov, S. E. Kupriyanov, and N. N. Tunitskii, Zh. Eksp. Teor. Fiz. **46**, 833 (1964) [Sov. Phys.—JETP **19**, 570 (1964)].

[30]S. M. Younger (private communication).